# Design of Peptoid Analogue Dimers and Measure of Their Affinity for Grb2 SH3 Domains†

M. Vidal,‡,§ W.-Q. Liu,‡,§ C. Lenoir,§ J. Salzmann, N. Gresh,§ and C. Garbay*,§

*Département de Pharmacochimie Moléculaire et Structurale, INSERM U266, CNRS FRE 2463, UFR des Sciences Pharmaceutiques et Biologiques, 4, Avenue de l'Observatoire, 75270 Paris Cedex 06, France*

*Received December 5, 2003; Revised Manuscript Received March 25, 2004*

ABSTRACT: This paper describes the design of the highest affinity ligands for Grb2 SH3 domains reported so far. These compounds were designed by combining *N*-alkyl amino acid incorporation in a proline-rich sequence with subsequent dimerization of the peptoid sequence based on structural data and molecular modeling. Optimization of the linker size is discussed, and the *N*-alkyl amino acid incorporation into both monomeric halves is reported. Because the affinity for Grb2 of the optimized compounds was too high to be measured using the fluorescent modifications that they induce on the Grb2 emission spectrum, a competition assay was developed. In this test, Grb2 is pulled down from a cellular extract by the initial VPPPVPPRRR peptide bound to Sepharose beads. In the presence of competitors, the test quantifies the amount of Grb2 displaced from the beads. It has enabled us to determine a $K_i$ value in the $10^{-10}$ M range for the highest affinity Grb2 peptoid analogue dimer.

Grb2[1] (growth factor receptor-bound protein 2) is the most extensively studied adaptor protein involved in growth factor-stimulated signaling pathways (*1*, *2*). It is constituted by one SH2 (Src homology 2) domain surrounded by two SH3 domains. Grb2 binds tyrosine-phosphorylated proteins by means of its SH2 domain and interacts with several proline-rich motifs containing proteins through its SH3 domains (*3*). Sos, the nucleotide exchange factor for Ras (*4*, *5*), is the most important ligand of Grb2 SH3 domains. Thus, the recruitment of Grb2-Sos at the membrane promotes Ras GTP loading and subsequent stimulation of the mitogen-activated protein (MAP) kinase cascade involved in the control of cell growth and differentiation (*4*, *6*−*9*). Anarchic proliferation observed in leukemia and several cancers has been related to the dysfunction of receptors or intracellular proteins with tyrosine kinase activity, coupled to p21 Ras activation (*10*−*12*).

To provide antiproliferative agents, synthetic phosphotyrosine-containing peptides were designed that inhibit the interaction between the SH2 domain of Grb2 and either RTKs or adaptators such as Shc with $IC_{50}$ values in the $10^{-8}$−$10^{-9}$ M range (*13*, *14*). Another approach, which consists of inhibiting the interaction between Sos and the two SH3 domains of Grb2, was also developed in our laboratory (*15*). Thus, to attain simultaneous interactions with both SH3 domains of Grb2, peptidimers have been designed by coupling two proline-rich sequences from Sos using linkers of different sizes. Some of these peptides have shown very high affinities for Grb2, with $K_d$ values in the $10^{-8}$ M range, and are able to inhibit Grb2−Sos interaction in vitro. In this paper, we describe an approach developed in order to design novel dimers, with increased affinities for Grb2. After having optimized the length of the linker, we were able to further improve the Grb2 binding affinities of peptidimers by introducing N-alkylated residues on each monomeric half. The resulting analogues contain valines and arginines which are not N-alkylated. As such, they are not actual peptoids. We therefore will denote them as "peptoid analogues". Because the affinity values of such dimers for Grb2 were too strong to be evaluated with a fluorometric measurement (*15*), we have developed, on a cellular extract, a competition assay between Grb2 and the VPPPVPPRRR sequence loaded on Sepharose beads. This assay, based on proline-rich peptide pull-down experiments, provided a measure of inhibition concentrations ($IC_{50}$ values) for each competitor, which allowed calculating $K_i$ inhibition constants. The test was validated by the good similarity observed of $K_i$ values measured for the VPPPVPPRRR sequence and its dimer as compared to $K_d$ measurement by fluorescence. It allowed to measure for a peptoid−dimer complexed to Grb2

† This work was supported by the Ligue Nationale Contre le Cancer, Comité de Paris.

* To whom correspondence should be addressed. Tel: (33) 1 42 86 40 80. Fax: (33) 1 42 86 40 82. E-mail: christiane.garbay@univ-paris5.fr.

‡ These authors contributed equally to thi work.

§ Present address: Laboratoire de Pharmacochimie Moléculaire et Cellulaire, INSERM U648, CNRS FRE 2718, UFR Biomédicale des Saints Pères, 45, Rue des Saints Pères, 75270 Paris Cedex 06, France.

[1] Abbreviations: AcOH, acetic acid; Aha, 6-aminohexanoic acid; Alloc, allyloxycarbonyl; Boc, *tert*-butyloxycarbonyl; DAP, 2,3-diaminopropionic acid; DCC, *N*,*N*′-dicyclohexylcarbodiimide; DIEA, diisopropylethylamine; DIC, diisopropylcarbodiimide; DMAP, 4-(dimethylamino)pyridine; DMF, *N*,*N*-dimethylformamide; DMSO, dimethyl sulfoxide; DTT, dithiothreitol; ER22, epidermal growth factor receptor overexpressing clone 22; EVH1, Ena-VASP protein homology domain 1; Fmoc, 9-fluorenylmethyloxycarbonyl; Grb2, growth factor receptor-bound protein 2; GTP, guanosine triphosphate; HOBt, 1-hydroxybenzotriazole; HPLC, high-performance liquid chromatography; $IC_{50}$, inhibitory concentration 50; MAP kinase, mitogenic-activated protein kinase; NMM, *N*-methylmorpholine; NMR, nuclear magnetic resonance; NMP, *N*-methylpyrrolidone; PTK, protein tyrosine kinase; pTyr or pY, phosphotyrosine; RTK, receptor protein tyrosine kinase; SH2, Src homology 2; SH3, Src homology 3; Shc, SH2 domain containing adaptor protein; Sos, son of sevenless; TFA, trifluoroacetic acid; TFFH, tetrafluoroformamidinium hexafluorophosphate; TIPS, triisopropylsilane.

10.1021/bi030252n CCC: $27.50 
Published on Web 05/21/2004

a subnanomolar $K_i$ value. The use of the present test could be generalized to quantify affinity constants for the formation of exceptionally tight-binding ligand−receptor complexes. Finally, molecular modeling has unraveled new ligand−Grb2 interactions occurring along the surface of the SH3 platforms that provided a structural explanation for the increase of Grb2 affinity.

## MATERIALS AND METHODS

*Fluorescence Experiments.* Grb2 was a gift from Dr P. Chardin (Nice, France). Fluorescence measurements were performed on a Perkin-Elmer fluorometer in a 10 × 10 mm cuvette at 25 °C with stirring. Briefly, the excitation was at 292 nm (band with 2.5 nm), and emission was recorded at 345 nm (band with 5 nm). The buffer was 50 mM Hepes, and 1 mM DTT, pH 7.5. Since the addition of high amounts of peptides also increased the final volume by a few percent, a correction was introduced to take the dilution factor into account in the corresponding experiments. The determination of Grb2−peptide equilibrium constants ($K_d$s) was performed, as described by Cussac et al. (*16*), assuming a simple bimolecular association.

Considering the equilibrium Grb2 + P ⇆ Grb2−P, one obtains the equation $[Grb2-P]^2 + [Grb2-P]\{y - [Grb2]_0 - K_d\} - [Grb2]_0 y = 0$,where $[Grb2]_0$ is the total concentration of active Grb2 and $y$ represents the added peptide concentration. Resolving such an equation leads to its determinant calculation: $\Delta = (y - [Grb2]_0 - K_d)^2 + 4[Grb2]_0 y$. ln the case of $[Grb2]_0 \gg K_d$, it is possible to approximate $y - [Grb2]_0 - K_d$ to $y - [Grb2]_0$, and we obtain the simplified expression for the $\Delta$ value $([Grb2]_0 + y)^2$. Derived solutions for the initial equation are then $[Grb2-P] = [Grb2]_0$ or $[Grb2-P] = y$. When $y < [Grb2]_0$, $[Grb2-P]$ is directly proportional to $y$ (all free Grb2 present in solution is immediately complexed upon dimer addition: $[Grb2-P] = y$) and when $y > [Grb2]_0$, all Grb2 is consumed and $[Grb2-P] = [Grb2]_0$. Consequently, since fluorescence changes $\Delta F$ are directly related to the fraction of the Grb2−P complex, the representation of $\Delta F = f(y)$ in the case of $[Grb2]_0 \gg K_d$ will be constituted by two straight lines crossing one another at a point corresponding to $y = [Grb2]_0$. So, in these conditions, no $K_d$ determination was possible as described for the peptoid analogue dimers **11** and **12** in this paper.

*Antibodies.* The anti-Grb2 antibody was purchased from Santa Cruz Biotechnology Laboratories (Santa Cruz, CA). The secondary antibody coupled to peroxidase was from Amersham.

*Cells and Preparation of Cell Lysates.* Adherent ER22 cells (hamster fibroblasts overexpressing the human epidermal growth factor receptor) were a gift from Dr. J. Pouyssegur, France. They were routinely grown and lyzed at the subconfluence state as described in Vidal et al. (*40*). The same stock solution of cellular extract was used for all of the competition experiments.

*Peptide Coupling to Sepharose Beads.* One milligram of the peptide derived from the Sos sequence (VPPPVPPRRR) was coupled to 1 mL of CNBr-activated Sepharose 4B (Pharmacia, Piscataway, NJ), according to Hermanson et al. (*41*).

*Competition between Grb2/VPPPVPPRRR Bead Association.* VPPPVPPRRR beads (30 μL) were incubated overnight at 4 °C with 20 μg of cell lysate in the presence of the inhibitory peptide at the appropriate concentration. Beads were washed four times (15 min) with PBS and 0.01% Tween 20 at 4 °C. Affinity-precipitated proteins were eluted by boiling sodium dodecyl sulfate sample buffer for 5 min and submitted to SDS−polyacrylamide gel electrophoresis.

*Immunoblotting Experiments.* As we have already described (*40*), Grb2-precipitated protein was submitted to a western blot and revealed by the enhanced chemiluminescence method (ECL, Amersham).

*$K_i$ Calculation.* In the competition test allowing the determination of $IC_{50}$, the interaction between Grb2 and the VPPPVPPRRR peptide loaded on Sepharose beads is quite comparable to the interaction between a radioligand and its receptor, and it is possible to calculate a $K_i$ value since the affinity ($K_d$) of the VPPPVPPRRR sequence for Grb2 is known (18 μM). In these conditions, according to the Cheng−Prusoff relation (*34*), $K_i = IC_{50}/(1 + L/K_d)$, where $IC_{50}$ denotes the value of the competitor concentration able to displace 50% of the interaction (determined by the competition test), $L$ the concentration of the displaced ligand, and $K_d$ its affinity for Grb2 (18 μM).

Since VPPPVPPRRR is able to displace the interaction between Grb2 and the VPPPVPPRRR peptide loaded on Sepharose beads with an $IC_{50} = 358 \pm 22$ μM, this means that the peptide concentration $L$ has the same value (considering that beads have no influence for the interaction). So, the expression of $L/K_d$ is 358/18 = 19.9 and the $K_i$ value is $IC_{50}/(1 + 19.89)$. For the VPPPVPPRRR peptide, $K_i$ = 358/20.9 = 17.1 μM. This value is in the same magnitude order of the $K_d$ value of VPPPVPPRRR (18 μM) for Grb2 through the fluorescent test and allowed us the calculation of $K_i$ values for all of the competitors. These values are simply calculated by the relation $K_i = IC_{50}/20.9$ for each competitor.

*Chemistry.* The synthesis of peptides was carried out by using the stepwise solid-phase method of Merrifield on an Applied Biosystems (ABI) 431A automated peptide synthesizer with small-scale Fmoc chemistry. For the symmetric peptide dimers, Fmoc-Lys(Fmoc)-OH or Fmoc-DAP(Fmoc)-OH was loaded on the HMP resin by DCC/DMAP. After deprotection of both Fmoc groups of the lysine residue by a solution of 20% piperidine in NMP, residues of spacers (Aha) and both of the proline-rich sequences were prolonged simultaneously by subsequent DCC/HOBt coupling. Concerning the asymmetric peptide dimers, Fmoc-Lys(Alloc)-OH was used in place of Fmoc-Lys(Fmoc)-OH. After deprotection of the Fmoc group and introduction of the first peptide sequence, with the last N-terminal residue in Boc form on the α-$NH_2$ group of the linker lysine, the Alloc protecting group of the side chain ε-$NH_2$ of lysine was removed by 3 equiv of $Pd(PPh_3)_4$ in 8 mL of $CHCl_3$/AcOH/NMM (37/2/1) for 2 h under nitrogen at room temperature. The second proline-rich sequence was then introduced on the side chain of lysine. For the synthesis of N-alkylated peptide dimers, the Fmoc-Lys(Fmoc)-OH was loaded on the HMP resin. The first four residues of the proline-rich sequence were coupled by DCC/HOBt and the Fmoc groups removed by piperidine. The bromoacetic acid was then added by double coupling using DIC in DMF. The bromides were then substituted by a 2 M solution of (*S*)-(α-phenyl)ethylamine in DMSO with a repetition. The valine residues were coupled by double

coupling with TFFH/DIEA in DMF. The remaining residues were introduced by the DCC/HOBt coupling.

Peptides were then deprotected and cleaved from the resin by treatment with 10 mL of TFA/$H_2O$/TIPS (9.50/0.25/0.25 in volume) for 3 h at room temperature. The filtrates from the cleavage reactions were evaporated and precipitated in cold ether. The peptide precipitates were collected by centrifugation and washed several times with cold ether. Crude peptides were purified by reverse-phase HPLC on a Vydac $C_{l8}$ column (5 $\mu$m, 250 $\times$ 10 mm) using acetonitrile gradients with 0.1% of TFA. The molecular weight of peptides were verified by ion electrospray mass spectrometry.

*Molecular Modeling.* Molecular modeling used the Discover software from Accelrys (Accelrys, Inc.) and the AMBER force field (*40*). A distance-dependent dielectric constant of 4 was used ($\epsilon = 4r$). The peptidimer was fully relaxed, as well as the side chains of the protein. We started from the structure initially derived in our laboratory for the standard peptidimer (*15*) and substituted Pro4 on both N-terminal sides by *N*-alkylglycine. A first round of constrained energy minimization was done by enforcing overlap of the modified peptidimer with the standard one, followed by unconstrained energy minimization. A similar procedure was applied to yield the antiparallel complex, after rotating by 180°, using computer graphics, the peptidimer around an axis grossly perpendicular to the main direction of the SH3 domains. The main chain atoms of the Grb2 protein were frozen in the first docking stage, and up to 6000 steps of energy minimization with the BFGS algorithm were performed. In the last step, energy minimization was resumed, with additional relaxation of the main chain atoms of the protein residues involved in peptidimer binding. Convergence was attained with rms derivative values of $10^{-4}$.

## RESULTS

*Proline-Rich Sequence Optimization.* It was previously described that Sos, which interacts with Grb2 through its C-terminal region (*6*), contained different PXΦPXR consensus proline-rich sequences (Φ = hydrophobic amino acid, X = any amino acid) required for SH3 domain type II recognition (*3*, *16*). Their affinity for Grb2 had been measured by fluorescence. Proline-rich peptides have been docked following NMR data (*17*−*19*) at the surface of the three-dimensional structure of Grb2 determined from X-ray (*20*). Thus, we observed that the carboxylate moieties of the peptides were in a relatively close proximity, namely, in the 10 Å range. Therefore, as a first step, we linked two such proline-rich sequences through the carboxyl groups. The linker was constituted by two aminohexanoic acid residues (Aha) connected via their carboxylate to the two amino groups of a lysine to provide sufficient flexibility for a better adaptation of the two proline-rich sequences at the surface of the Grb2−SH3 domains. Dimer **2** containing VPPPVPPRRR and PESPPLLPPR, two sequences found in Sos, was compared to the monomer **1**, VPPPVPPRRR, by affinity measurement through fluorescence. As shown in Table 1, dimer **2** exhibits a $K_d$ value of 300 nM for Grb2, as compared to 18 $\mu$M in the case of monomer VPPPVPPRRR. This increased affinity suggests a simultaneous interaction of peptidimer **2** with both SH3 domains of Grb2. This was confirmed by the much lower affinities measured between Grb2 and control peptides, where the second proline-rich sequence was either deleted (compound **3**, $K_d$ = 17 $\mu$M) or replaced by the same but scrambled proline-rich sequence (peptidimer **4**, $K_d$ = 14 $\mu$M), devoid of the consensus PXΦPXR motif. These results validate the development of the dimerization approach for increasing the affinity for Grb2 of proline-rich peptides. Since, the monomeric VPPPVPPRRR sequence exhibited the higher affinity for both C- and N-SH3 domains of Grb2 (*16*), dimer **5**, constituted by two identical VPPPVPPRRR sequences, was synthesized and shown to exhibit a very high affinity for Grb2 with a $K_d$ dissociation constant of 50 nM.

Table 1: Peptide Affinities for Grb2 ($K_d$ Values in $\mu$M): Influence of Proline-Rich Sequence and Linker Size[a]

| | Peptide sequence | $K_d$(μM) |
|---|---|---|
| **1** | VPPPVPPRRR | 18±1.1 (*15*) |
| **2** | VPPPVPPRRR - Aha - K - COOH<br>\|<br>PESPPLLPPR - Aha | 0.3 ± 0.05 |
| **3** | VPPPVPPRRR - Aha - K - COOH<br>\|<br>Aha | 17 ± 1 |
| **4** | VPPPVPPRRR - Aha - K - COOH<br>\|<br>EPPPSRLPLP - Aha | 14 ± 1 |
| **5** | VPPPVPPRRR - Aha - K - COOH<br>\|<br>VPPPVPPRRR - Aha | 0.05 ± 0.005 |
| **6** | VPPPVPPRRR - K - COOH<br>\|<br>VPPPVPPRRR - Aha | 0.04 ± 0.005 |
| **7** | VPPPVPPRRR - K - COOH<br>\|<br>VPPPVPPRRR | 0.04±0.005 (*15*) |
| **8** | VPPPVPPRRR - DAP - COOH<br>\|<br>VPPPVPPRRR | N.M. |

[a] The affinities of the proline-rich peptides for Grb2 have been measured using a fluorescence test and are expressed as $K_d$ (dissociation constant) values (in $\mu$M). NM: not measurable. We observed a strong variation of fluorescence, but it was impossible to obtain a fit with classical mathematical models of 1/1 or 1/2 peptide/Grb2 interaction.

*Linker Length Optimization.* The first chosen linker was constituted by one lysine and two aminohexanoic acids in order to provide both flexibility and symmetry for interacting with both SH3 domains. Since this connector having two aminohexanoic groups (compound **5**) appeared, on the basis of preliminary molecular modeling, a little too long, we decided to optimize the length of the connector. Therefore, only one aminohexanoic acid was added with the lysine (compound **6**), and a connector made out of a lysine alone (compound **7**) was tested as well. The distance between the two carboxyl groups amounting to 10 Å, lysine alone as linker, appeared a priori too short to optimally connect two peptides that were individually docked along the surface of the two SH3 domains. Nevertheless, lysine-connected peptidimer **7** was endowed with the same affinity for Grb2 as compound **6**.

Molecular modeling of compound **7** complexed with Grb2 shows only limited deformations of Grb2, possibly explaining its high affinity (*15*).

We have next evaluated the effect of reducing the length of the connecting lysine side chain in such a way as to avoid bis-interaction. Reduction of the dimer connector length was obtained by introducing a 2,3-diaminopropionic acid residue (molecule **8** in Table 1) in place of the lysine. In this amino acid, the side chain has only two methylene groups instead of four as in a lysine. Therefore, if the shorter DAP was used instead of Lys as a linker, spanning of both SH3 domains of one Grb2 protein by the dimer would be prevented, and one could expect a 1/1 or a 1/2 stoichiometry of the complex. Upon addition of the DAP-linked peptidimer to Grb2, a variation of fluorescence was observed. However, analysis of the signal (Enzfit software; see ref *21*) did not fit classical mathematical models of either 1/1 or 1/2 peptide/Grb2 complexes. This result shows that the shorter dimer does not bind Grb2 according to a standard model in which each monomer spans one SH3 domain. Considering the short length of the DAP side chain, this dimer is hypothesized to interact with the two SH3 domains of Grb2 according to a "flip-flop" mechanism (*22*−*24*). Thus there would be one Pro-rich sequence bound in alternation to the C-SH3 or to the N-SH3 domain of Grb2 in a rapid oscillatory movement.

Taken together, all these results show the lysine side chain to have an appropriate length as a connector enabling a peptidimer to span both Grb2 SH3 domains. It was then retained for the design of novel peptoid dimers with optimized affinity for Grb2.

*Novel Dimers with Very High Affinity for Grb2. (A) Dimer Design.* Previous NMR studies (*17*−*19*) showed that, in the proline-rich peptide V**P**PP**V**PP**R**RR complexed with the N-SH3 domain of Grb2, residues **P**, **V**, and **R** of the peptide were mostly involved through a combination of hydrophobic as well as electrostatic interactions with the SH3 domain recognition platform. Proline residues of the SH3 binding core PXXP motif (denoted as sites $P_2$ and $P_{-1}$, as numbered with respect to residue **V**) are very important to give rise to the polyproline type II helix conformation of the peptide that is essential for its interaction with SH3 domains. Subsequent replacement by other amino acids constitutes one further critical step in the search for pseudopeptidic analogues of proline-rich sequences. The prolines of the SH3 core PXXP motif are critical because alanine or other amino acid replacements are not tolerated at these locations. However, proline residue replacement is acceptable as long as N-substitution is maintained (*3*, *25*−*31*). By a combinatorial method, the consequences of introducing N-alkylated amino acids in the consensus sequence to provide additional interactions with the SH3 domain have been studied. This yielded ligands that selectively bound SH3 domains among which one had a very high affinity for the Grb2 N-SH3 domain. Thus in the YEVPPPV**P**PRRR Sos-derived sequence, residue **P** was replaced by (*S*)-(α-phenyl)ethylglycine (peG), resulting in a peptoid analogue YEVPPPV(**peG**)-PRRR having a $K_d$ value of 40 nM for the Grb2 N-SH3 domain (*30*). Along these lines, we also mention the recent work by Zimmermann et al. which has designed "peptomer" ligands of the Ena-VASP protein homology domain 1 involved in several actin-based motility processes (*32*). These authors have shown that replacement of the highly conserved residues **F** and **P** of EVH1 ligand SFE**FP**PPPTEDEL by N-alkylated glycines could occur without impairing their EVH1 binding affinities. This further supports the feasibility of designing peptoid analogues that involve proline-rich sequences to interfere with protein−protein interactions. A similar approach, using N-substituted glycine peptoids led to peptoid trimers with biological activity and the discovery of high-affinity $\alpha_1$-adrenergic and $\mu$-opiate seven-transmembrane G-coupled receptor ligands (*33*). We have adapted such a strategy to design N-alkylated peptidimers, replacing this proline residue on each monomeric half.

Table 2: N-Alkylated Monomer Affinities for Grb2 and Its Isolated SH3 Domains[a]

| | peptide | N-SH3 | C-SH3 | whole Grb2 |
|---|---|---|---|---|
| **1** | VPPPVPPRRR | 2.6 ± 0.2 | 40 ± 5 | 18 ± 2[b] |
| **9** | YEVPPPV(peG)PRRR | 0.40 ± 0.07 | 7 ± 1.5 | 1.80 ± 0.40 |
| **10** | VPPPV(peG)PRRR | 0.55 ± 0.16 | 3.27 ± 0.48 | 2.40 ± 0.40 |

[a] The affinities of the proline-rich peptides were measured using a fluorescence test and are expressed as $K_d$ (dissociation constant) values (in $\mu$M). [b] Reference *15*.

As a first step, the two monomers YEVPPPV(peG)PRRR and VPPPV(peG)PRRR were synthesized, and their affinity was measured for each of the two individual SH3 domains of Grb2 and for the whole Grb2 protein. The two SH3 domains were themselves synthesized by solid-phase synthesis (*17*). The affinity measurements are summarized in Table 2. The original peptide VPPPVPPRRR (**1**) exhibits $K_d$ values for N-SH3, C-SH3, and Grb2 of respectively 2.6, 40, and 18 $\mu$M. On the other hand, the N-alkylated derived peptides exhibit $K_d$ values that are 1 order of magnitude smaller. As shown in Table 2, both peptoid analogues YEVPPPV(peG)PRRR (**9**) and VPPPV(peG)PRRR (**10**) show $K_d$ values in the same order of magnitude for the individual N-SH3 domain of respectively 0.40 and 0.55 $\mu$M. In the case of the C-SH3 domain, compounds **9** and **10** have $K_d$ values of 7.00 and 3.27 $\mu$M, respectively. This order-of-magnitude difference is probably due to the optimization of this peptide by Nguyen et al. with respect to the N-SH3 domain of Grb2, rather than for the C-SH3 one (*30*). Similar to the case of the VPPPVPPRRR (**1**) sequence, $K_d$ values of the peptoid analogues for the whole Grb2 protein are intermediate between those for the N- and C-SH3 isolated domains. The following step, toward further enhancing ligand affinity for Grb2, has consisted of the construction of peptoid analogue dimers upon dimerizing either VPPPV(peG)PRRR or YEVPPPV(peG)PRRR sequences with the lysine as linker, whose side chain length was found above to be adequate. All results were compared to the symmetric standard dimer $(VPPPVPPRRR)_2K$ (**7**).

*(B) Grb2 Inhibitor Affinity Measurement: Limitations of the Fluorescent Method.* All dissociation constants ($K_d$) measured by fluorescence are summarized in Table 3. As already described, dimerization of the VPPPVPPRRR sequence induced a strong increase of the affinity for Grb2, amounting to 18 $\mu$M for VPPPVPPRRR **1**, as compared to 0.04 $\mu$M for the corresponding dimer **7**. Typical fluorescence experiments are given in Figure 1 for the peptoid analogue monomer (Figure 1A) and the corresponding dimer (Figure 1B). It was possible to access through a curve with asymptotic shape to the affinity of the monomer VPPPV-

Table 3: Peptide Affinities for Grb2[a]

| | peptide | $K_d$ ($\mu$M) | $IC_{50}$ ($\mu$M) | $K_i$ ($\mu$M) |
|---|---|---|---|---|
| **1** | VPPPVPPRRR | $18 \pm 2$[b] | $358 \pm 22$ | $17.1 \pm 3.8$ |
| **7** | $(VPPPVPPRRR)_2K$ | $0.040 \pm 0.005$ | $0.8 \pm 0.1$ | $0.038 \pm 0.011$ |
| **8** | $(VPPPVPPRRR)_2DAP$ | NM[c] | $582 \pm 48$ | $27.8 \pm 6.8$ |
| **9** | YEVPPPV(peG)PRRR | $1.80 \pm 0.40$ | ND[d] | ND |
| **10** | VPPPV(peG)PRRR | $2.40 \pm 0.40$ | $32 \pm 2$ | $1.53 \pm 0.35$ |
| **11** | $(VPPPV(peG)PRRR)_2K$ | NM | $0.0050 \pm 0.0008$ | $(0.20 \pm 0.08) \times 10^{-3}$ |
| **12** | $(YEVPPPV(peG)PRRR)_2K$ | NM | ND | ND |

[a] $K_d$ were measured by fluorescence. $IC_{50}$ have been measured by the competition test. These values are expressed in micromolar. According to the Cheng−Prussoff equation (see Materials and Methods), it was possible to calculate $K_i$ values, allowing the best comparison between all molecules. [b] Reference *15*. [c] NM: not measurable. [d] ND: not determined.

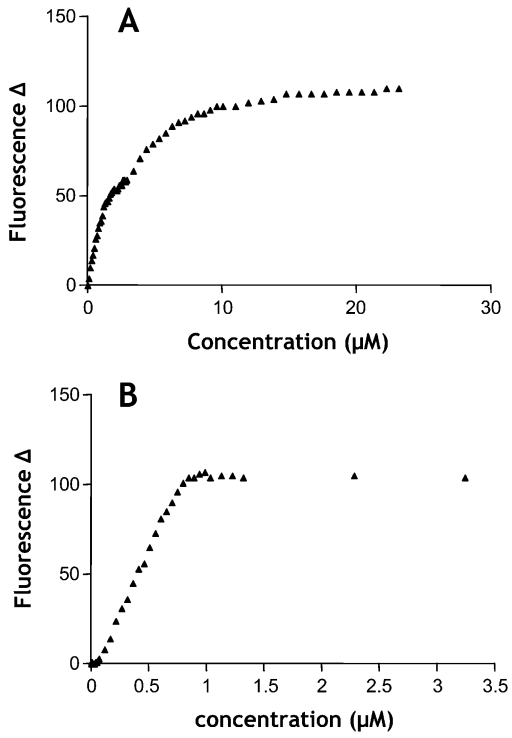


FIGURE 1: Typical fluorescence results obtained with either VPPPV(peG)PRRR (A) or $[VPPPV(peG)PRRR]_2K$ (B). The curves represent $\Delta F$, the relative fluorescence variation compared to the initial fluorescence of Grb2 and corrected by a factor corresponding to the dilution induced by peptide addition, as a function of final peptide concentration. Grb2 initial concentration was 1 $\mu$M. The experiment was carried out in 50 mM Hepes buffer, pH 7.5, and 1 mM DTT. In a typical experiment, using the VPPPV(peG)PRRR (**10**) monomer, we have obtained a curve with an asymptotic shape (panel A). In the case of $[VPPPV(peG)PRRR]_2K$ (**11**) (panel B), a titration curve was obtained. Binding is saturated at 1 $\mu$M, corresponding to Grb2 concentration, showing that the affinity of the peptide is too high to be measured (see text and Materials and Methods).

(peG)PRRR (Figure 1A, $K_d = 2.4$ $\mu$M). Under the same conditions the affinity of the peptoid analogue dimer was correspondingly increased. In fact, the increase was so high that the binding affinity of the corresponding dimers could not be assayed by a standard fluorescence test. Thus, two straight lines, crossing one another at a point corresponding to the Grb2 concentration in the measurement solution, were obtained (Figure 1B) instead of a classical curve (Figure 1A). Under these conditions, all free Grb2 present in solution is immediately complexed upon peptide addition, and the curve obtained is a titration curve. Binding is saturated at 1 $\mu$M, corresponding to Grb2 concentration, showing that the affinity of the peptoid analogue dimer is too high to be measured by this method. Our conclusion is that the dimeric peptoid analogues exhibit largely stronger affinities for Grb2 than the classical dimer.

*Grb2 Inhibitor Affinity Measurement: Competition Test Development. (A) Peptide and Peptidimer.* The results of the preceding section prompted us to develop another test to determine the affinity of the peptoid analogue dimer for Grb2. To avoid the use of a radioactive probe, we based our test on a previous result in which we showed that the VPPPVPPRRR peptide from Sos loaded on CNBr-activated Sepharose beads was able to pull down Grb2 from cellular extract (*15*). The test thus consists of a displacement, using potential SH3 domain binders, of the Grb2 pull down on VPPPVPPRRR-loaded beads. After protein complex degradation and electrophoresis, Grb2 was revealed by specific western blot. The relative intensities of the corresponding bands were quantified to obtain an estimation of $IC_{50}$ values (Figure 2). Since our previous results had shown that the additional tyrosine and glutamic residues were not essential to optimize Grb2−SH3 interactions (Table 2), we have developed our test on the VPPPV(peG)PRRR **10** peptoid and its dimerized analogue as competitors to inhibit the interaction taking place between the VPPPVPPRRR **1** sequence loaded on Sepharose beads and Grb2 from a cellular extract. The VPPPVPPRRR **1** sequence and its dimerized analogues having either a lysine (**7**) or a DAP (**8**) residue as a linker were also tested. In these experiments, increasing concentrations of competitor peptides were added to a cellular lysate of exponentially growing ER22 cells. Figure 2 shows characteristic blots obtained in these experiments (Figure 2A) and the relative intensities of the corresponding bands (Figure 2B).

Figure 2A shows that both VPPPVPPRRR **1** and $(VPPPV-PPRRR)_2K$ **7**, used as control, are able to displace Grb2 bound to VPPPVPPRRR peptide loaded on Sepharose beads. The evaluated $IC_{50}$ values for these two Grb2−SH3 domain inhibitors are $358 \pm 22$ and $0.8 \pm 0.1$ $\mu$M, respectively (Figure 2B). These results confirm the existence of a 2 order-of-magnitude difference in the relative capacities of these molecules to bind Grb2, as already described by our group (*15*) and as reported in Table 3.

*(B) Effect of Linker Length Reduction.* The dimer linked with DAP instead of a lysine (compound **8**) is also able in our competition assay to displace Grb2 from VPPPVPPRRR loaded on Sepharose beads (Figure 2A). Nevertheless, the estimated $IC_{50}$ value is $582 \pm 48$ $\mu$M (Figure 2B). This result shows that dimerization with a short linker results in a decrease of the affinity for Grb2, with respect to that of the monomeric peptide.

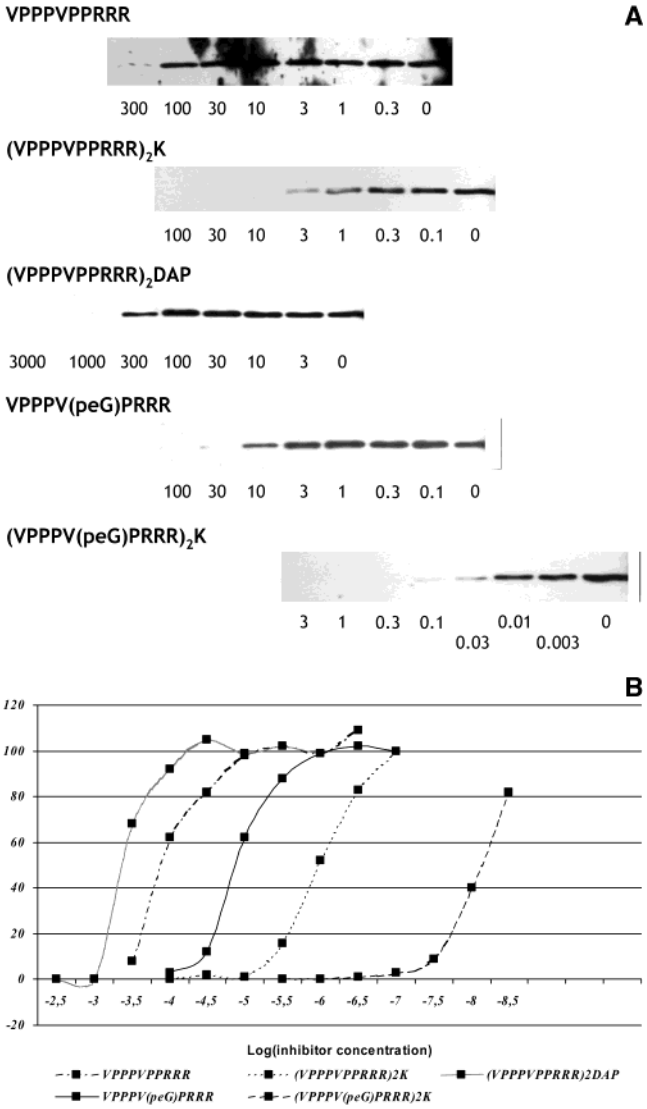


FIGURE 2: Displacement of the interaction of Grb2/VPPPVPPRRR loaded on Sepharose beads by Grb2 SH3 domain inhibitors. (A) VPPPVPPRRR beads were incubated with ER22 lysates in the presence of inhibitory peptide at the appropriate concentration ($\mu$M). Affinity-precipitated proteins were submitted to a SDS−PAGE and anti-Grb2 western blot. The dimerization of either VPPPVPPRRR or VPPPV(peG)PRRR with a lysine residue as a linker highly increased their affinities for Grb2. Such results were obtained with three independent experiments. (B) Quantification of the band intensities to evaluate $IC_{50}$ values of inhibitors. Band intensities were quantified using a Bio-Profil V6.0 Vilber-Lourmat (Marne la Vallée, France). This quantification confirms the fact that [VPPPV-(peG)PRRR]$_2$K (**11**) is the most potent inhibitor for Grb2 SH3 domains, exhibiting an $IC_{50}$ in this test around 5 nM.

*(C) The Peptoid Analogue Dimer Can Inhibit the Interaction between VPPPVPPRRR and Grb2 with a Very High Efficiency.* As expected, monomeric peptoid VPPPV(peG)-PRRR **10** is able to displace the VPPPVPPRRR/Grb2 interaction with higher efficiency than the monomeric VPPPVPPRRR **1** (Figure 2A). The estimated $IC_{50}$ values are $32 \pm 2$ $\mu$M for the N-alkylated analogue VPPPV(peG)PRRR **10** as compared to $358 \pm 22$ $\mu$M for VPPPVPPRRR **1** (Figure 2B and Table 3). This is consistent with the corresponding 1 order-of-magnitude difference on $K_d$ values for Grb2. Dimerization of the alkylated peptoid (compound **11**) induces a strong increase in its ability to displace Grb2 from VPPPVPPRRR beads (Figure 2A). The estimated $IC_{50}$ for this peptoid−dimer is approximately 5 nM, i.e., a 2 order-of-magnitude decrease with respect to the classical dimer (Figure 2B). This result is totally in accordance with fluorescence results which anticipated a strong affinity increase compared to the monomeric sequence **1**.

*(D) Inhibition Constant ($K_i$) Determination.* The interaction between Grb2 and the VPPPVPPRRR peptide loaded on Sepharose beads is comparable to the interaction between a ligand and its receptor. In this case, it is possible to access $K_i$ calculations from $IC_{50}$ values using the Cheng−Prusoff equation: $K_i = IC_{50}/(1 + L/K_d)$ (*34*). This enables the determination of $K_i$ for dimers whose affinities are too high to be measured by the fluorescent method. Results are expressed in micromolar in Table 3. When monomer **1**, which in our test is coupled to Sepharose beads, is used as a competitor, it exhibits a $K_i$ value of $17.1 \pm 3.8$ $\mu$M. Such a value is fully consistent with the $K_d$ measured by fluorescence for Grb2 (18 $\mu$M) (Table 2), enabling us to apply this calculation method to all other inhibitors. Standard dimer **7** exhibits a $K_i$ of $38 \pm 11$ nM, and the N-alkylated monomer **10** has a $K_i$ of $1.53 \pm 0.35$ $\mu$M. These values are consistent with the $K_d$ ones that were measured by the fluorescence test (dimer **7**, $K_d = 40 \pm 5$ nM; monomer **10**, $K_d = 2.4 \pm 0.4$ $\mu$M). N-Alkylated dimer **11**, for which $K_d$ measurement was not possible by fluorescence, exhibits a $K_i$ of $0.20 \pm 0.08$ nM; namely, a subnanomolar $K_d$ value is expected. Conversely, compound **8**, in which the Lys connector was replaced by DAP, undergoes an affinity decrease, namely, a $K_i$ value of $27.8 \pm 6.8$ $\mu$M.

*Molecular Modeling Results.* There are no high-resolution X-ray crystallography data presently available for the complex of dimers with Grb2. Our experiments to obtain a cocrystallization of Grb2 with peptidimer were unsuccessful. The size of Grb2, emcompassing both SH3 and the SH2 domain (217 residues), is too large to lend itself to a 2D NMR study of its complex with ligands. In fact, such NMR studies were limited so far to the complex of a single SH3 domain with a proline-rich dodecapeptide (*17*−*19*). In the absence of such information, molecular modeling can provide insight into the complementary ligand−Grb2 interactions that can take place at the atomic level. This technique has thus recently enabled us to predict the structure of the complex formed between a bisphosphotyrosine-containing peptide and the SH2 domain of Grb2 (*13*), the most important features of which were subsequently confirmed by X-ray crystallography (*35*). We comment below on the results of energy minimization of the structure of the complex formed between Grb2 and the peptoid analogue dimer **11**.

Two orientations were considered, according to whether the monomer that is N-terminal to the lysine connector interacts with the N-terminal SH3 domain of Grb2 (parallel orientation) or whether it interacts with the C-terminal SH3 domain (antiparallel orientation). Accordingly, the monomer linked to the N$\epsilon$ of the lysine side chain interacts with the C- or with the N-terminal SH3 domain in these two respective orientations. The antiparallel orientation was shown to give rise to the strongest stabilization energies, as it enables to maximize the number of ionic interactions of the central Arg residues of the peptoid analogue dimer with Glu and Asp residues at the interface between the two SH3 domains. The proposed complex between the peptoid analogue dimer and Grb2 is represented in Figure 3A. The

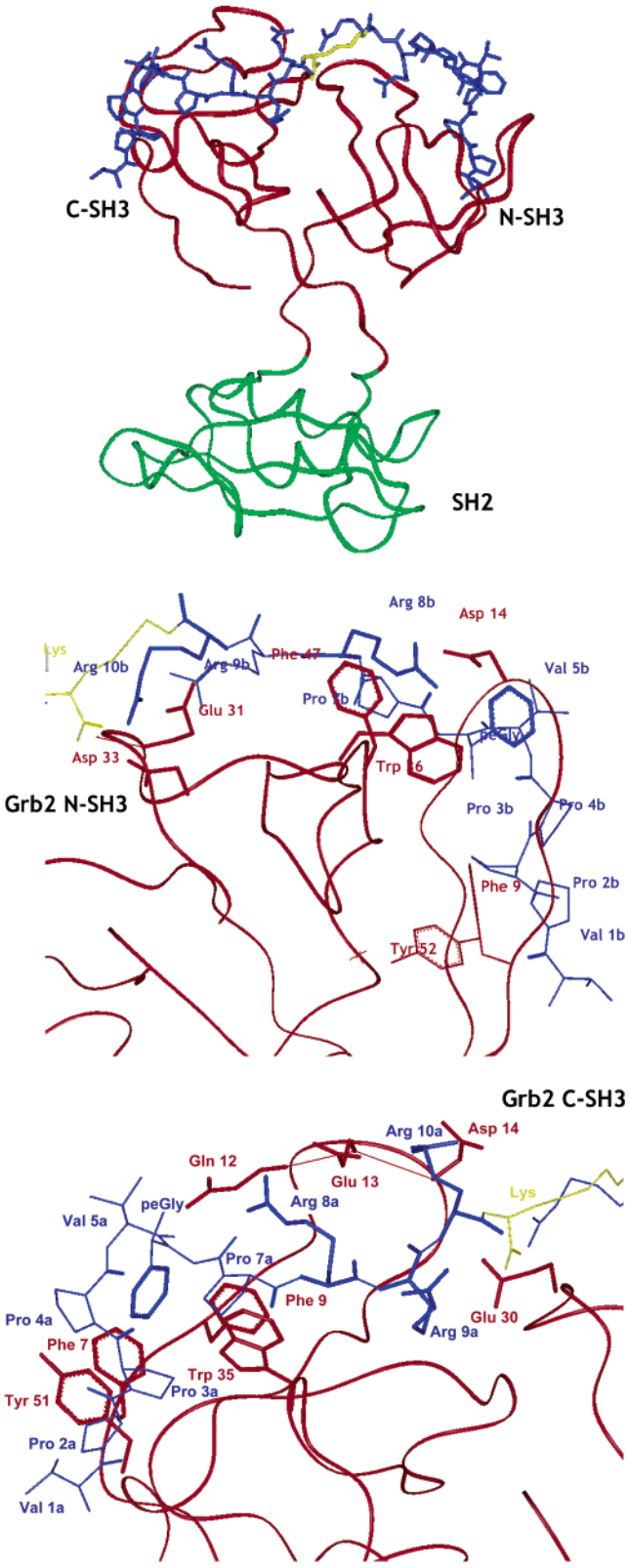


FIGURE 3: Complex modeling between Grb2 and [VPPPV(peG)-PRRR]$_2$K. (A) Model of the Grb2−peptoid−dimer **11** complex showing that the polyproline helices (blue) and lysine linker (yellow) of the peptidimer can interact with both N- and C-SH3 domains (red) of Grb2. The SH2 domain is in green. (B) Details of interactions of compound **11** with the N-SH3 domain (see text for discussion). (C) Details of interactions of compound **11** with the C-SH3 domain (see text for discussion).

interactions with the N-SH3 and the C-SH3 domains are highlighted in panels B and C of Figure 3, respectively. Amino acids of the peptoid analogue dimer labeled with a and b below are those interacting with the C- and the N-terminal domains, respectively. On the N-SH3 domain (Figure 3B), the ionic interactions involve Arg8b of the dimer with Asp14 on one hand, Arg9b with Glu31 on the other hand, and Arg10b with both Glu31 and Asp33. In addition, Arg8b is simultaneously in a parallel cation−$\pi$ interaction with Phe47 and in a T-like cation−$\pi$ interaction with Trp36 of the N-terminal SH3. On the C-SH3 domain (Figure 3C), these interactions are between Arg8a and both Gln12 and Glu13, between Arg9a and Glu30 (bidentate), and between Arg10a and both Glu13 and Asp14. While most interactions involving residues Pro2a and Pro2b characterized for our originally designed peptidimer with the hydrophobic platform of SH3 domains are retained (*15*), the phenyl group of the alkylated residue (peG) on each monomer interacts with aromatic sites of the bound SH3 domain. These are residue Trp36 on the N-terminal domain and residues Phe7, Phe9, Trp35, and Tyr51 on the C-terminal SH3. Such additional interactions should contribute to the enhancement of the binding affinity upon passing from standard peptidimer **7** to the N-alkylated one **11** (Table 2).

## DISCUSSION

This paper reports the design of novel peptoid analogue dimers with subnanomolar affinities for Grb2−SH3 domains. Only two approaches modifying proline-rich sequences so far resulted in significant affinity enhancements. The first one had incorporated N-alkylated residues in the proline-rich sequences (*30*), and the second consisted in dimerization of proline-rich peptides (*15*). The approach that we report here combines both modifications and gives rise to N-alkylated proline-rich peptoid dimers endowed with the highest affinities for Grb2 SH3 domains that have been reported to date. We have also in the course of this study developed a test that should enable to quantify $K_i$ values for exceptionally tightly bound complexes that could not lend themselves to standard $K_i$ determinations.

In the first part of this paper, we show that a lysine residue constitutes the optimal connector for peptidimers, thereby allowing simultaneous targeting of both SH3 domains of Grb2. If a diaminopropionic acid (DAP) residue instead of a lysine one is used, the dimer's affinity decreases to values comparable to, and even smaller than, those of the monomers of the series.We have hypothesized a flip-flop mechanism to be involved which might account for the fact that the observed fluorescence variation did not fit a classical l/l or 1/2 peptide/Grb2 model. Such a mechanism had already been described for other ligands (*22*−*24*).

In our case, the comparison of competition experiment results obtained with the monomer and this dimer indicated a slight decrease of efficiency for the dimer, suggesting that if a flip-flop mechanism occurs in this interaction, it would not be sufficient to stabilize the complex. A short linker might in fact prevent simultaneous optimal in-register interactions of each monomer with its targeted SH3.

In a second part of the paper, we report the design of peptoid analogue dimers with very high affinity for Grb2. Nguyen et al. (*30*) had shown that replacement of one proline residue in the YEVPPPVPPRRR peptide enhances the affinity for the Grb2 N-SH3 domain and published a $K_d$ value

of 40 nM. In our experimental conditions through fluorescence assay, a $K_d$ value of 400 nM was obtained. Such a variation can easily be explained by different buffers used in experimental conditions, and this is supported by the sensitivity of the complexes to ionic strength.

Nguyen et al. (*30*) had shown that the YEVPPPV(peG)-PRRR sequence is highly specific for the Grb2 N-SH3 domain, as compared to other SH3 domains. Here, we clearly show that the specificity between the two SH3 domains of Grb2 is not significantly higher in the case of the YEVPPPV-(peG)PRRR sequence than for the VPPPVPPRRR one. Thus, the C-SH3/N-SH3 $K_d$ ratio is respectively 18 for VPPPVP-PRRR **1** and 15 for YEVPPPV(peG)PRRR **9** (Table 2). This specificity seems to decrease in the absence of the two additional residues tyrosine and glutamic acid in the case of VPPPV(peG)PRRR **10** ($K_d$ ratio C-SH3/N-SH3 = 7). Despite the weak Grb2−SH3 specificity of the VPPPVPPRRR monomeric sequence, we have demonstrated that the peptidimer **7** has a high specificity for Grb2 (*15*). This could arise from the onset of simultaneous interactions with both SH3 domains of Grb2, the linker length being adequate so that each monomer would not interfere with the binding of the other. In the case of the peptoid analogue dimer, molecular modeling has, in addition, shown the occurrence of additional interactions of its two *N*-alkylbenzyl substituents with aromatic residues on each SH3 domain. Such interactions should account for the enhancement of the binding affinities upon changing from the peptidic sequence to the peptoid one and complement the ionic interactions of its arginine residues with glutamate and aspartate residues on both domains. The results reported in Figure 2 show that the peptoid analogue dimer **11** exhibits a $K_i$ of about 0.2 nM as compared to 38 nM for the standard peptidimer **7**, namely, a 2 order-of-magnitude ratio. Using bis-N-alkylated peptoids obtained through the combinatorial chemistry approach of Nguyen et al. (*31*), dimerization could possibly also provide compounds with further enhancements of Grb2 binding affinities.

In the third part, we have developed a competition assay based on Grb2 pull-down experiments. The displacement by competitor peptides of the Grb2/VPPPVPPRRR-loaded complex allows to measure the peptide affinities for Grb2 (Figure 2). The evaluation of $K_i$ by this displacement test enables to bypass the use of a radioligand and simplifies the experiments. These results support the fact that $K_i$ values can be extracted from $IC_{50}$ determinations. It can be noted that systematic $K_i$ determinations should facilitate comparison of literature data. We are presently developing a two-step ELISA test based on this approach, which will allow to rapidly screen inhibitors derived from chemical libraries.

Finally, we propose potential interactions between Grb2 and compound **11**, from molecular modeling, that may account for increased affinity and serve as a hypothesis to develop new inhibitors of Grb2/Sos interactions.

In conclusion, our data demonstrate that compounds capable to recognize with both enhanced affinity and selectivity Grb2 SH3 domains can be tailored by dimerization. To our knowledge, this is the first time that molecules in a subnanomolar range are reported as binders for the Grb2−SH3 domains. Such dimers have affinities of the same order of magnitude and even higher than those reported for protein−protein interactions and might provide promising inhibitors of the Grb2 signaling pathway.

Moreover, the design of specific inhibitors of Grb2−SH3 domains can lead to both pharmacological tools to help deciphering signal transduction (*36*, *37*) and design of potential therapeutic agents in cancerology. In this connection, we have already shown that peptidimer $(VPPPVPPRRR)_2K$, upon coupling with a vectorizing peptide, displayed cellular activity in ex vivo tests (*15*). The 100-fold higher affinity of the present N-alkylated dimer could be anticipated to give rise to corresponding enhancements of its chemotherapeutic potential. Since several peptoids are cell penetrating, such as analogues of the highly basic Tat (49−57) sequence (RKKRRQRRR) based polycationic peptoid (*38*, *39*), we have tested the biological ability of our molecules having three arginine residues in the monomer sequence and six in the dimer one on the cellular model without any carrier. No effect was observed, while the vectorized classical dimer was active (*15*). Thus, to enhance bioavailability, we are presently synthesizing vectorized N-alkylated derivatives using the antennapedia sequence as the carrier, as already described for molecule **7** (*15*).

## ACKNOWLEDGMENT

The molecular modeling studies reported in this work were performed on the computers of the Centre Inter-regional de l'Enseignement Supérieur (CINES, Montpellier, France), whose support is gratefully acknowledged. We thank Jean Marie Zajac for helpful discussions on $K_i$ calculations. We also thank G. Pieffet for molecular modeling experiments performed during his DEA.

## REFERENCES

1. Lowenstein, E. J., Daly, R. J., Batzer, A. G., Li, W., Margolis, B., Lammers, R., Ullrich, A., Skolnik, E. Y., Bar-Sagi, D., and Schlessinger, J. (1992) The SH2 and SH3 domain-containing protein Grb2 links receptor tyrosine kinases to ras signaling, *Cell 70*, 431−442.
2. Chardin, P., Cussac, D., Maignan, S., and Ducruix, A. (1995) The Grb2 adaptor, *FEBS Lett. 369*, 47−51.
3. Simon, J. A., and Schreiber, S. L. (1995) Grb2 SH3 binding to peptides from Sos: Evaluation of a general model for SH3-ligand interactions, *Chem. Biol. 2*, 53−60.
4. Buday, L., and Downward, J. (1993) Epidermal growth factor regulates p21ras through the formation of a complex of receptor, Grb2 adapter protein, and Sos nucleotide exchange factor, *Cell 73*, 611−620.
5. Rozakis-Adcock, M., Fernley, R., Wade, J., Pawson, T., and Bowtell, D. (1993) The SH2 and SH3 domains of mammalian Grb2 couple the EGF receptor to the Ras activator mSos1, *Nature 363*, 83−85.
6. Chardin, P., Camonis, J. H., Gale, N. W., van Aelst, L., Schlessinger, J., Wigler, M. H., and Bar-Sagi, D. (1993) Human Sos1: a guanine nucleotide exchange factor for Ras that binds to GRB2, *Science 260*, 1338−1343.
7. Egan, S. E., Giddings, B. W., Brooks, M. W., Buday, L., Sizeland, A. M., and Weinberg, R. A. (1993) Association of Sos Ras exchange protein with Grb2 is implicated in tyrosine kinase signal transduction and transformation, *Nature 363*, 45−51.
8. Li, N., Batzer, A., Daly, R., Yajnik, V., Skolnik, E., Chardin, P., Bar-Sagi, D., Margolis, B., and Schlessinger, J. (1993) Guanine-nucleotide-releasing factor hSos1 binds to Grb2 and links receptor tyrosine kinases to Ras signalling, *Nature 363*, 85−88.
9. Skolnik, E. Y., Batzer, A., Li, N., Lee, C.-H., Lowenstein, E., Mohammadi, M., Margolis, B., and Schlessinger, J. (1993) The function of GRB2 in linking the insulin receptor to Ras signaling pathways, *Science 260*, 1953−1955.
10. Gishizky, M. L., Johnson-White, J., and Witte, O. N. (1993) Evaluating the effect of P210 BCR/ABL on growth of hemato-

poietic progenitor cells and its role in the pathogenesis of human chronic myelogenous leukemia, *Semin. Hematol. 30*, 6−8.
11. Pandey, P., Kharbanda, S., and Kufe, D. (1995) Association of the DF3/MUC1 breast cancer antigen with Grb2 and the Sos/Ras exchange protein, *Cancer Res. 55*, 4000−4003.
12. Sastry, L., Cao, T., and King, R. (1997) Multiple Grb2-protein complexes in human cancer cells, *Int. J. Cancer 70*, 208−213.
13. Liu, W.-Q., Vidal, M., Gresh, N., Roques, B. P., and Garbay, C. (1999) Small peptides containing phosphotyrosine and adjacent αMe-phosphotyrosine or its mimetics as highly potent inhibitors of Grb2 SH2 domain, *J. Med. Chem. 42*, 3737−3741.
14. Gay, B., Suarez, S., Caravatti, G., Furet, P., Meyer, T., and Schoepfer, J. (1999) Selective GRB2 SH2 inhibitors as anti-Ras therapy, *Int. J. Cancer 83*, 235−241.
15. Cussac, D., Vidal, M., Leprince, C., Liu, W.-Q., Cornille, F., Tiraboschi, G., Roques, B. P., and Garbay, C. (1999) A Sos-derived peptidimer blocks the Ras signaling pathway by binding both Grb2 SH3 domains and displays antiproliferative activity, *FASEB J. 13*, 31−38.
16. Cussac, D., Frech, M., and Chardin, P. (1994) Binding of the Grb2 SH2 domain to phosphotyrosine motifs does not change the affinity of its SH3 domains for Sos proline-rich motifs, *EMBO J. 13*, 4011−4021.
17. Goudreau, N., Cornille, F., Duchesne, M., Parker, F., Tocqué, B., Garbay, C., and Roques, B. P. (1994) NMR structure of the N-terminal SH3 domain of Grb2 and its complex with a proline-rich peptide from Sos, *Nat. Struct. Biol. 1*, 898−907.
18. Terasawa, H., Kohda, D., Hatanaka, H., Tsuchiya, S., Ogura, K., Nagata, K., Ishii, S., Mandiyan, V., Ullrich, A., Schlessinger, J., and Inagaki, F. (1994) Structure of the N-terminal SH3 domain of GRB2 complexed with a peptide from the guanine nucleotide releasing factor Sos, *Nat. Struct. Biol. 1*, 891−897.
19. Wittekind, M., Mapelli, C., Lee, V., Goldfarb, V., Friedrichs, M. S., Meyers, C. A., and Mueller, L. (1997) Solution structure of the Grb2 N-terminal SH3 domain complexed with a ten-residue peptide derived from SOS: direct refinement against NOEs, J-couplings and 1H and 13C chemical shifts, *J. Mol. Biol. 267*, 933−952.
20. Maignan, S., Guilloteau, J. P., Fromage, N., Arnoux, B., Becquart, J., and Ducruix, A. (1995) Crystal structure of the mammalian Grb2 adaptor, *Science 268*, 291−293.
21. Leatherbarrow, R. J. (1987) ENZFIT, Elsevier Biosoft, Cambridge.
22. Le Pecq, J. B., Le Bret, M., Barbet, J., and Roques, B. P. (1975) DNA polyintercalating drugs: DNA binding of diacridine derivatives, *Proc. Natl. Acad. Sci. U.S.A. 72*, 2915−2919.
23. Shuker, S. B., Hajduk, P. J., Meadows, R. P., and Fesik, S. W. (1996) Discovering high-affinity ligands for proteins: SAR by NMR, *Science 274*, 1531−1534.
24. Li, L., Tang, X., Taylor, K. G., DuPré, D. B., and Yappert, M. C. (2002) Conformational characterization of ceramides by nuclear magnetic resonance spectroscopy, *Biophys. J. 82*, 2067−2080.
25. Cohen, G. B., Ren, R., and Baltimore, D. (1995) Modular binding domains in signal transduction proteins, *Cell 80*, 237−248.
26. Sparks, A. B., Quilliam, L. A., Thorn, J. M., Der, C. J., and Kay, B. K. (1994) Identification and characterization of Src SH3 ligands from phage-displayed random peptide libraries, *J. Biol. Chem. 269*, 23853−23856.
27. Sparks, A. B., Rider, J. E., Hoffman, N. G., Fowlkes, D. M., Quillam, L. A., and Kay, B. K. (1996) Distinct ligand preferences of Src homology 3 domains from Src, Yes, Abl, Cortactin, p53bp2, PLCgamma, Crk, and Grb2, *Proc. Natl. Acad. Sci. U.S.A. 93*, 1540−1544.
28. Rickles, R. J., Botfield, M. C., Zhou, X.-M., Henry, P. A., Brugge, J. S., and Zoller, M. J. (1995) Phage display selection of ligand residues important for Src homology 3 domain binding specificity, *Proc. Natl. Acad. Sci. U.S.A. 92*, 10909−10913.
29. Grabs, D., Slepnev, V. I., Songyang, Z., David, C., Lynch, M., Cantley, L. C., and De Camilli, P. (1997) The SH3 domain of amphiphysin binds the proline-rich domain of dynamin at a single site that defines a new SH3 binding consensus sequence, *J. Biol. Chem. 272*, 13419−13425.
30. Nguyen, J. T., Turck, C. W., Cohen, F. E., Zuckermann, R. N., and Lim, W. A. (1998) Exploiting the basis of proline recognition by SH3 and WW domains: Design of N-substituted inhibitors, *Science 282*, 2088−2092.
31. Nguyen, J. T., Porter, M., Amoui, M., Miller, W. T., Zuckermann, R. N., and Lim, W. A. (2000) Improving SH3 domain ligand selectivity using a nonnatural scaffold, *Chem. Biol. 7*, 463−473.
32. Zimmermann, J., Kuhne, R., Volkmer-Engert, R., Jarchau, T., Walter, U., Oschkinat, H., and Ball, L. J. (2003) Design of N-substituted peptomer ligands for EVH1 domains, *J. Biol. Chem. 278*, 36810−36818.
33. Zuckermann, R. N., Martin, E. J., Spellmeyer, D. C., Stauber, G. B., Shoemaker, K. R., Kerr, J. M., Figliozzi, G. M., Goff, D. A., Siani, M. A., Simon, R. J., Banville, S. C., Brown, E. G., Wang, L., Richter, L. S., and Moos, W. H. (1994) Discovery of nanomolar ligands for 7-transmembrane G-protein-coupled receptors from a diverse N-(substituted)glycine peptoid library, *J. Med. Chem. 37*, 2678−2685.
34. Cheng, Y. C., and Prusoff, W. H. (1973) Relationship between the inhibition constant ($K_1$) and the concentration of inhibitor which causes 50% inhibition ($I_{50}$) of an enzymatic reaction, *Biochem. Pharmacol. 22*, 3099−3108.
35. Nioche, P., Liu, W.-Q., Broutin, I., Charbonnier, F., Latreille, M.-T., Vidal, M., Roques, B. P., Garbay, C., and Ducruix, A. (2002) Crystal structures of the SH2 domain of Grb2: highlight on the binding of a new high-affinity inhibitor, *J. Mol. Biol. 315*, 1167−1177.
36. Saci, A., Liu, W.-Q., Vidal, M., Garbay, C., Rendu, F., and Bachelot-Loza, C. (2002) Differential effect of the inhibition of Grb2-SH3 interactions in platelet activation induced by thrombin and by Fc receptor engagement, *Biochem. J. 363*, 717−725.
37. Carlier, M. F., Nioche, P., Broutin-L'Hermite, I., Boujemaa, R., Le Clainche, C., Egile, C., Garbay, C., Ducruix, A., Sansonetti, P., and Pantaloni, D. (2000) GRB2 links signaling to actin assembly by enhancing interaction of neural Wiskott-Aldrich syndrome protein (N-WASp) with actin-related protein (ARP2/3) complex, *J. Biol. Chem. 275*, 21946−21952.
38. Wender, P., Mitchell, D. J., Pattabiraman, K., Pelkey, E. T., Steinman, L., and Rothbard, J. B. (2000) The design, synthesis, and evaluation of molecules that enable or enhance cellular uptake: peptoid molecular transporters, *Proc. Natl. Acad. Sci. U.S.A. 97*, 13003−13008.
39. Peretto, I., Sanchez-Martin, R. M., Wang, X.-H., Ellard, J., Mittoo, S., and Bradley, M. (2003) Cell penetrable peptoid carrier vehicles: synthesis and evaluation, *Chem. Commun.*, 2312−2313.
40. Vidal, M., Montiel, J.-L., Cussac, D., Cornille, F., Duchesne, M., Parker, F., Tocqué, B., Roques, B. P., and Garbay, C. (1998) Differential interactions of the growth factor receptor-bound protein 2 N-SH3 domain with son of sevenless and dynamin: Potential role in the Ras-dependent signaling pathway, *J. Biol. Chem. 273*, 5343−5348.
41. Hermanson, G. T., Mallia, A. K., and Smith, P. K. (1992) *Immobilized affinity ligand techniques*, pp 53−56, Academic Press, New York.
42. Weiner, S. J., Kollman, P. A., Nguyen, D. T., and Case, D. A. (1986) An all-atom force-field for simulations of proteins and nucleic acids, *J. Comput. Chem. 7*, 230−252.

BI030252N